

# EFFECT OF THE ACID-BASE PROPERTIES OF Mg-Al MIXED OXIDES ON THE CATALYST DEACTIVATION DURING ALDOL CONDENSATION REACTIONS

V.K. DÍEZ, C.R. APESTEGUÍA and J.I. DI COSIMO\*

*Instituto de Investigaciones en Catálisis y Petroquímica -INCAPE- (UNL-CONICET).*

*Santiago del Estero 2654, (3000) Santa Fe, Argentina.*

*e-mail: dicosimo@fiqus.unl.edu.ar*

**Abstract**— The effect of chemical composition of Mg-Al mixed oxides on both the acid-base properties and the deactivation process during the gas phase self-condensation of acetone was studied. The activity and selectivity for acetone oligomerization depended on the catalyst acid-base properties. Mg-rich catalysts selectively yielded mesityl oxides whereas Al-rich  $Mg_yAlO_x$  oxides produced mainly isophorone. The initial deactivation rate, increased linearly with the density of surface basic sites, thereby suggesting that although  $Mg_yAlO_x$  oxides promote the self-condensation of acetone by both acid- and base-catalyzed mechanisms, the deactivation rate would be closely related to the surface basic properties. The  $Mg_yAlO_x$  activity declines in the acetone oligomerization reaction due to a blockage of both base and acid active sites by a carbonaceous residue formed by secondary reactions. The amount and the nature of the carbon deposits were characterized by temperature-programmed oxidation technique.  $Mg_yAlO_x$  and  $Al_2O_3$  formed more and heavier coke than pure MgO but the latter deactivates faster. The deactivation rate and coke composition are defined by the nature of the active site involved in the coke-forming reactions at different catalyst compositions rather than by the carbon amount or polymerization degree.

**Keywords**— Catalyst Deactivation, Acetone Oligomerization, Acid-Base Catalysis

## I. INTRODUCTION

Mg-Al mixed oxides obtained by thermal decomposition of anionic clays of hydrotalcite structure, present acidic or basic surface properties depending on their chemical composition (Di Cosimo *et al.*, 2000). These materials contain the metal components in close interaction thereby promoting bifunctional reactions that are catalyzed by Brønsted base-Lewis acid pairs. Among others, hydrotalcite-derived mixed oxides promote aldol condensations (Reichle, 1985), alkylations (Velu and Swamy, 1996) and alcohol eliminations (Di Cosimo *et al.*, 2000). In particular, we

have reported that Mg-Al mixed oxides efficiently catalyze the gas-phase self-condensation of acetone to  $\alpha,\beta$ -unsaturated ketones such as mesityl oxides and isophorone (Di Cosimo *et al.*, 1998a). Unfortunately, in coupling reactions like aldol condensations, basic catalysts are often deactivated either by the presence of byproducts such as water in the gas phase or by coke build up through secondary side reactions. Deactivation has traditionally limited the potential of solid basic catalysts to replace environmentally problematic and corrosive liquid bases. However, few works in the literature deal with the deactivation of solid bases under reaction conditions. Studies relating the concerted and sequential pathways required in the deactivation mechanism with the acid-base properties of the catalyst surface are specially lacking. In this work, we studied the deactivation of Mg-Al mixed oxides in the gas phase oligomerization of acetone. We prepared and characterized calcined Mg-Al hydrotalcites with Mg/Al atomic ratios of 1-9. The effect of composition on both the surface and catalytic properties as well as the catalyst deactivation were investigated by combining several characterization methods with catalytic data.

## II. METHODS

### A. Synthesis Procedures

Mg/Al hydrotalcite with Mg/Al atomic ratios ( $\gamma$ ) of 1, 3, 5 and 9 were prepared by coprecipitation of  $Mg(NO_3)_2 \cdot 6H_2O$  and  $Al(NO_3)_3 \cdot 9H_2O$  at 333 K and pH = 10. After drying overnight at 348 K, precursors were decomposed in  $N_2$  at 673 K in order to obtain the  $Mg_yAlO_x$  mixed oxides. More experimental details are given elsewhere (Di Cosimo *et al.*, 2000). Reference samples of  $Al_2O_3$  and MgO were prepared following the same procedure.

### B. Methods for the Sample Characterization

The crystalline structure of the samples was determined by powder X-ray diffraction (XRD) methods. Acid site densities were measured by temperature-programmed desorption (TPD) of  $NH_3$  preadsorbed at room temperature. The structure of  $CO_2$  chemisorbed on hydrotalcite-derived samples was determined by infrared spectroscopy (IR).  $CO_2$  adsorption site

\* To whom correspondence should be addressed

densities were obtained from TPD of CO<sub>2</sub> preadsorbed at 298 K. Total surface areas (S<sub>g</sub>) were measured by N<sub>2</sub> physisorption at 77 K.

### C. Acetone Self-Condensation Procedures

Self-condensation of acetone was carried out at 473 K and 100 kPa in a flow system with a differential fixed-bed reactor. Acetone was vaporized in H<sub>2</sub> (H<sub>2</sub>/acetone = 12) before entering the reaction zone. The standard contact time (W/F<sub>Acetone</sub><sup>0</sup>) was 49 g catalyst h/mole acetone. Main reaction products were mesityl oxides (MO's), isophorone (IP) and mesitylene (MES). Traces of phorone and light hydrocarbons were also identified.

Coke formed on the catalysts was characterized after reaction, ex-situ, in a temperature-programmed oxidation (TPO) unit. The TPO experiments were carried out in a microreactor loaded with 50 mg of catalyst and using a 3 % O<sub>2</sub>/N<sub>2</sub> carrier gas. Sample temperature was increased linearly from room temperature to 973 K at 10 K/min. The reactor exit gases were fed into a methanator operating at 673 K to convert CO<sub>x</sub> in methane and then analyzed by flame ionization detector.

## III. RESULTS AND DISCUSSION

### A. Catalyst Characterization

The hydroxycarbonate precursors showed diffraction patterns consistent with the layered double hydroxide structure proposed for hydrotalcite-like compounds, i.e., brucite-like sheets formed by OH groups and cations (Mg<sup>2+</sup> and Al<sup>3+</sup>) in octahedral coordination. Water molecules and charge-compensating CO<sub>3</sub><sup>2-</sup> anions are located in the interlayers. The hydrotalcite-like precursor composition is [Mg<sub>1-r</sub>Al<sub>r</sub>(OH)<sub>2</sub>]<sup>r+</sup>(CO<sub>3</sub>)<sub>r/2</sub><sup>2-</sup>·mH<sub>2</sub>O with  $r = \text{Al}/(\text{Al}+\text{Mg})$ ; the stoichiometric hydrotalcite compound, Mg<sub>6</sub>Al<sub>2</sub>(OH)<sub>16</sub>CO<sub>3</sub>·4H<sub>2</sub>O, is obtained for  $r = 0.25$ . Upon thermal decomposition at 673 K, the hydroxycarbonate precursors lose water and CO<sub>2</sub>. This

gaseous evolution develops a significant porous structure and gives rise to relatively high surface area mixed oxides as shown in Table 1. In the compositional range of this study, the analysis by XRD of the Mg<sub>y</sub>AlO<sub>x</sub> oxides showed only one crystalline phase, MgO periclase (ASTM 4-0829). No traces of hydrotalcite phases were detected after the thermal decomposition at 673 K.

Table 1 presents the acid and base site densities measured for all the samples by TPD of preadsorbed NH<sub>3</sub> and CO<sub>2</sub>, respectively. The base site density (n<sub>b</sub>) of the Mg<sub>y</sub>AlO<sub>x</sub> oxides was always between the values measured for MgO and Al<sub>2</sub>O<sub>3</sub>. Basic sites of different chemical nature were observed by FTIR of CO<sub>2</sub> and deconvolution of the CO<sub>2</sub> TPD traces; the strength of the basic sites follows the order: isolated low-coordination O<sup>2-</sup> ions > O<sup>2-</sup> in metal-oxygen pairs > OH groups (Di Cosimo *et al.*, 1998b). The density of metal-oxygen pairs measured by CO<sub>2</sub> TPD decreased with increasing the Al content at expenses of the surface hydroxylation.

The acid site density (n<sub>a</sub>), on the other hand, increases with increasing Al content. By deconvolution of the NH<sub>3</sub> TPD traces it was found that the Mg<sub>y</sub>AlO<sub>x</sub> oxides contain both Brønsted OH groups (low temperature peak) and Lewis acid sites provided by metal cations (high temperature peak) (Prinetto *et al.*, 2000; Berteau *et al.*, 1991). Since NH<sub>3</sub> adsorption was performed at room temperature, the measured Brønsted acidity may be attributed on all the samples to the reversible H-bonded NH<sub>3</sub> adsorption on surface hydroxyls. Lewis acidity of Mg<sub>y</sub>AlO<sub>x</sub> oxides corresponds to the irreversible coordinated NH<sub>3</sub> adsorption on surface defects with accessible Al<sup>3+</sup> cations whereas on alumina, the Lewis acidity was more likely assigned to Al<sup>3+</sup> cations in the abundant surface Al<sup>3+</sup>-O<sup>2-</sup> pairs. On MgO, on the other hand, the high temperature peak may result from the irreversible coordinated NH<sub>3</sub> adsorption on Mg<sup>2+</sup> cations combined with heterolytic dissociative adsorption leading to

**Table 1.** Chemical Composition, Crystalline Structure, Surface Area and Acid-Base Properties of Mg<sub>y</sub>AlO<sub>x</sub>, MgO and Al<sub>2</sub>O<sub>3</sub>.

Catalyst	$r = \text{Al}/(\text{Al}+\text{Mg})$ (molar) <sup>a</sup>	Crystalline Phase <sup>b</sup>	S <sub>g</sub> (m <sup>2</sup> /g)	Site Density (μmol/m <sup>2</sup> )	
				n <sub>b</sub> <sup>c</sup>	n <sub>a</sub> <sup>d</sup>
MgO	0.00	MgO	143	3.13	0.51
Mg <sub>9</sub> AlO <sub>x</sub>	0.11	MgO	114	1.17	0.81
Mg <sub>5</sub> AlO <sub>x</sub>	0.18	MgO	184	0.46	0.85
Mg <sub>3</sub> AlO <sub>x</sub>	0.24	MgO	238	0.59	1.02
Mg <sub>1</sub> AlO <sub>x</sub>	0.47	MgO	231	0.83	1.57
Al <sub>2</sub> O <sub>3</sub>	1.00	Amorphous	230	0.34	1.34

<sup>a</sup> by AAS; <sup>b</sup> by XRD; <sup>c</sup> by TPD of CO<sub>2</sub>; <sup>d</sup> by TPD of NH<sub>3</sub>

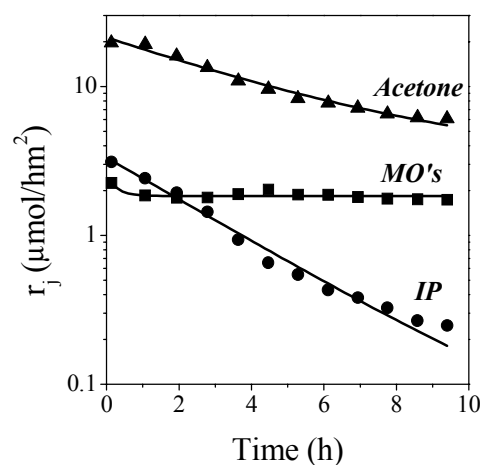


**Figure 1:** Time dependence of the acetone conversion and product formation rates on Mg<sub>9</sub>AlO<sub>x</sub> (T = 473 K, P<sub>Acetone</sub> = 7.7 kPa)

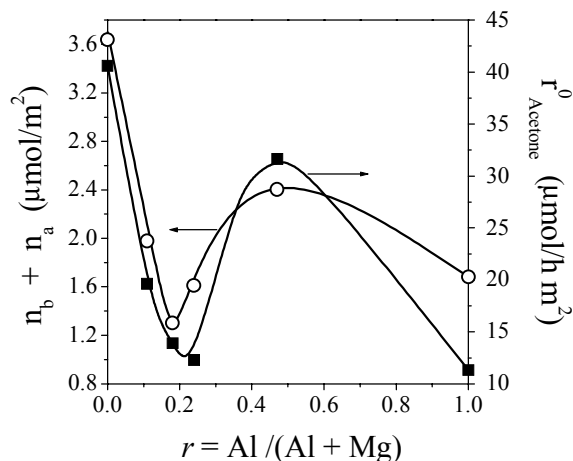


**Figure 2:** Initial acetone conversion rate and total number of active sites as a function of composition of  $\text{Mg}_y\text{AlO}_x$  oxides ( $T = 473 \text{ K}$ ,  $P_{\text{Acetone}} = 7.7 \text{ kPa}$ ,  $W/F^0_{\text{Acetone}} = 49 \text{ g h/mol}$ )

$\text{NH}_2^- - \text{H}^+$  species on  $\text{Mg}^{2+} - \text{O}^{2-}$  pairs (Garrone and Stone, 1985).

### B. Sample Composition, Surface Acid-Base Properties and Catalytic Activity

Acetone aldol condensation proceeds on either acidic or basic catalysts. On basic catalysts, the reaction products are mainly  $\alpha,\beta$ -unsaturated ketones (Di Cosimo *et al.*, 1996) whereas on acidic materials formation of aromatics and olefins is favored (Chang and Silvestri, 1977). In our catalytic tests, the main reaction products were mesityl oxides (MO's) and isophorone (IP). Over all the samples the reaction rate diminished as a function of time-on-stream as shown in Figure 1 for the

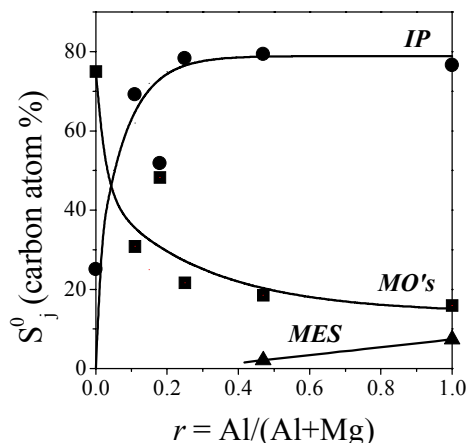


**Figure 3:** Initial product selectivity as a function of composition on  $\text{Mg}_y\text{AlO}_x$  catalysts ( $T = 473 \text{ K}$ ,  $P_{\text{Acetone}} = 7.7 \text{ kPa}$ ,  $X^0_{\text{Acetone}} = 12\text{-}14 \%$ )

$\text{Mg}_y\text{AlO}_x$  sample which lost about 60 % of its initial activity after 10 h-run. Initial reaction rates ( $r^0_j$ ) and product selectivities ( $S^0_j$ ) were calculated by extrapolating the reaction rates vs. time curves to zero.

In Figure 2 we have represented both the  $r^0_{\text{Acetone}}$  values and the total measured site density ( $n_T = n_b + n_a$ ) as a function of catalyst composition. Qualitatively, the variation of  $r^0_{\text{Acetone}}$  with increasing Al content is similar to that followed by  $n_T$  thereby suggesting that acetone conversion depends on both acid and base sites. Pure  $\text{MgO}$  was the most active catalyst whereas  $\text{Al}_2\text{O}_3$  showed the lowest activity. This is because Al-O pairs are much less active than Mg-O pairs for promoting the proton abstraction and carbanion stabilization steps

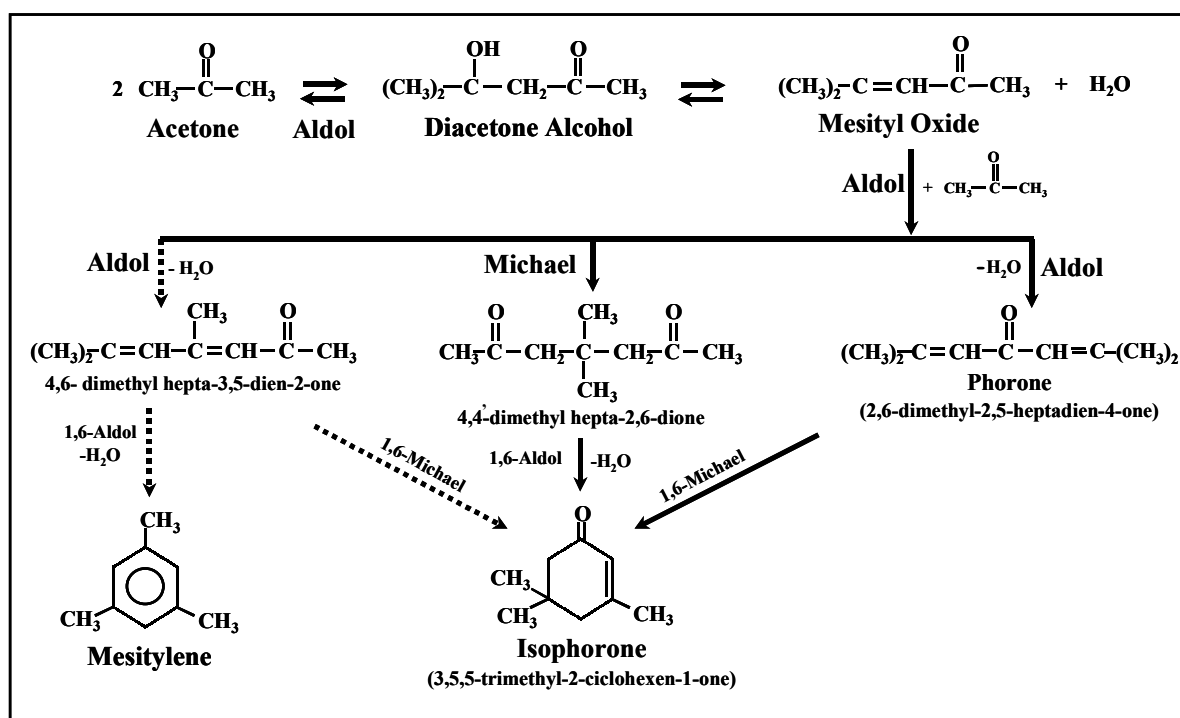


**Figure 4:** Acid- and base-catalyzed pathways for acetone conversion by aldol-like reactions on  $\text{Mg}_y\text{AlO}_x$  catalysts.

involved in aldol condensation reactions. We have shown (Di Cosimo *et al.*, 2000) that the aldolization rate is controlled on basic catalysts by the number of metal cation-oxygen anion surface pairs. Mg-rich  $Mg_yAlO_x$  oxides are less active than MgO because they exhibit a lower base site density and also poor acidic properties. In contrast, Al-rich  $Mg_yAlO_x$  oxides are more active than  $Al_2O_3$  due to a proper combination of acid and base sites.

In Figure 3 the initial product selectivities measured at isoconversion are represented as a function of catalyst composition. It is observed that the initial selectivities toward IP and MES increase with increasing the Al content whereas high selectivity toward MO's was obtained on Mg-rich catalysts. The presence of MES in low concentrations on Al-rich samples is indicative of an acid-catalyzed reaction pathway (Chang and Silvestri, 1977). Brønsted OH groups present on the surface of Al-rich catalysts, probably account for MES formation in accord with previous work (Di Cosimo *et al.*, 1998b) by X-ray photoelectron spectroscopy in which we demonstrated that in Al-rich  $Mg_yAlO_x$  mixed oxides, the binding energy of O 1s signal approached the values of surface OH groups thereby confirming a higher surface hydroxylation degree compared to Mg-rich catalysts.

Fig. 4 shows the main reaction scheme for the aldol condensation sequence leading to IP, where the dotted lines represent the reaction pathways to MES and IP formation that take place exclusively on acidic catalysts. The dimer, MO is the detected primary product formed by the initial self-condensation of acetone after fast dehydration of the unstable diacetone alcohol whereas IP is the final product arising from the consecutive aldol condensation between MO and acetone.

### C. Coke Formation and Characterization

In a previous work (Di Cosimo and Apesteguía, 1998), we found that MgO-based catalysts are deactivated during acetone oligomerization because of the formation of carbon deposits that block pores and surface active sites. Here, the coke formed on the samples after the 10-h catalytic runs was characterized by TPO technique. The TPO curves are shown in Figure 5 and quantitative

**Table 2.** Coke Characterization

Catalyst	TPO		TPO(N)	
	Carbon Amount (wt %)	Low-Temperature Peak (K)	Carbon Amount (wt %)	Peak Temperature (K)
MgO	12.5	623	4.7	730
$Mg_9AlO_x$	12.1	625	5.2	724
$Mg_5AlO_x$	13.6	650	5.5	736
$Mg_3AlO_x$	13.6	642	5.0	750
$Mg_1AlO_x$	22.4	697	7.6	760
$Al_2O_3$	15.8	709	6.0	787

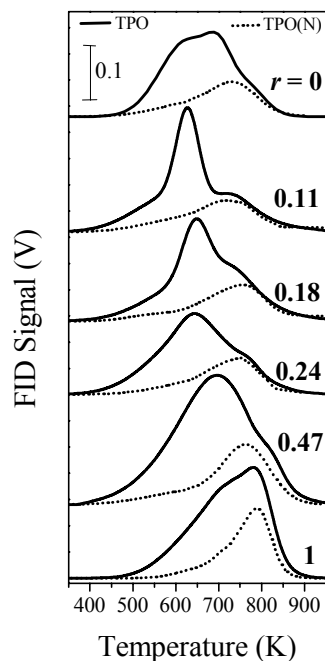


**Figure 5:** Coke burning experiments after acetone aldol condensation at 473 K on  $Mg_yAlO_x$  catalysts.  $r = Al/(Al + Mg)$

results are summarized in Table 2. The amount of carbon measured on the samples was between 12 and 22 wt. % and, as a general trend,  $Mg_yAlO_x$  and  $Al_2O_3$  formed more coke than pure MgO.

The TPO curves of Fig. 5 show the existence of two different carbon deposits; the main one gives a broad oxidation peak centered at 650-700 K (low-temperature peak); the other one arises as a shoulder at temperatures above 720 K (high-temperature peak). The low-temperature peak maximum shifts to higher temperatures with increasing Al content in the samples (Table 2). In order to obtain more insight on the nature of the carbon deposits, stripping experiments in pure  $N_2$  were carried out. In these experiments, coked samples were first treated in  $N_2$  from room temperature up to 973 K at 10 K/min before performing standard TPO runs. The TPO curves obtained after the  $N_2$  treatment are identified here as TPO(N) and are displayed in dotted lines in Fig. 5. The amount of carbon oxidized in TPO(N) experiments was between 4 and 8 wt % (Table 2). The shape and temperature maximum of the TPO(N) curves were similar to those of the high-temperature peaks in the corresponding TPO curves. These results show that the nitrogen treatment removes almost completely the carbon deposits that account for low-temperature peaks in TPO traces of Fig. 5. Both kind of carbon deposits seem to be related to the catalyst acid-base properties since both peak maxima gradually shifted to higher temperatures

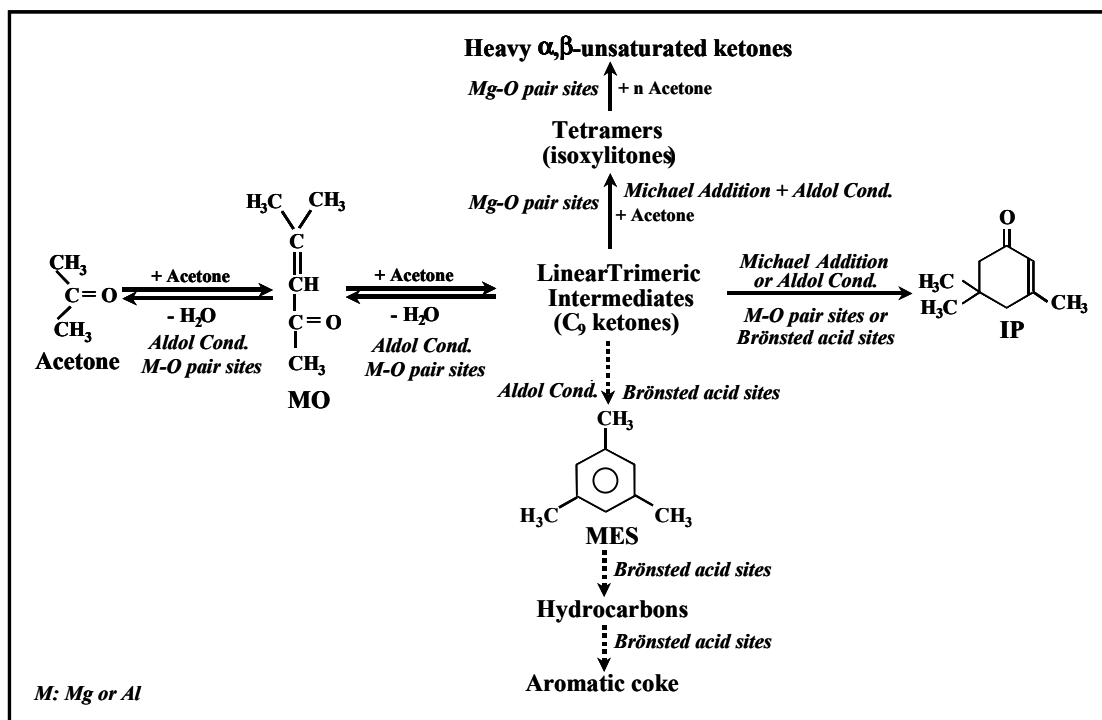


**Figure 6:** Coke-forming reactions during acetone oligomerization on  $Mg_3AlO_x$

at increasing Al contents as presented in Table 2.

In previous work (Di Cosimo and Apesteguía, 1998) we postulated that the coke precursor species on MgO-based catalysts are highly unsaturated linear compounds, such as 2,6-dimethylhepta-2,5-dien-4-one (phorone), 4,6-dimethylhepta-3,5-dien-2-one and 4,4'-dimethylhepta-2,6-dione which are trimeric compounds formed from MO and acetone by secondary aldol condensation reactions as shown in Figure 4. These linear trimers ( $C_9$  ketones) are non-detectable in the gas phase during reaction because they remain bound to the surface due to the strong interaction between the unsaturated chain and the basic centers. All of them are able to give IP by consecutive internal aldol or Michael

rearrangements (Reichle, 1980). Selective formation of one trimer in preference to the others depends on the catalyst acid-base properties. Phorone is the preferred intermediate on basic catalysts whereas formation of MES on acidic catalysts (Fig. 3) takes place only from 4,6-dimethylhepta-3,5-dien-2-one (Reichle, 1980). To obtain more information on the heavy compounds present in trace amounts in the gaseous products, we performed a GC-Mass Spectroscopy analysis of the reactor effluent collected in a condenser during acetone aldolization on  $Mg_1AlO_x$  catalyst. Besides acetone, MO's, IP and MES, we detected the trimer 4,6-dimethylhepta-3,5-dien-2-one ( $m/z = 138$ ), tetramers like isoxylitones ( $m/z = 178$ ) and also

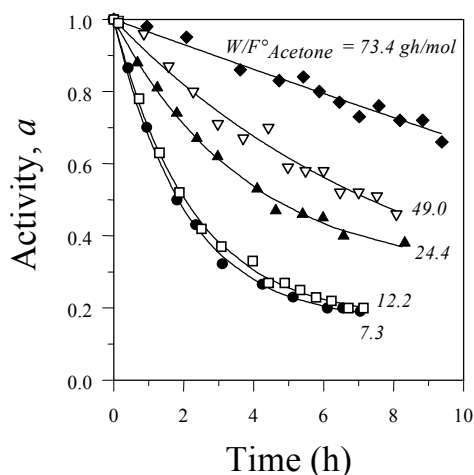


**Figure 7:** Acetone condensation activity as a function of time at different contact times ( $W/F^0_{Acetone}$ ) over MgO ( $T = 573$  K,  $P_{Acetone} = 7.7$  kPa)

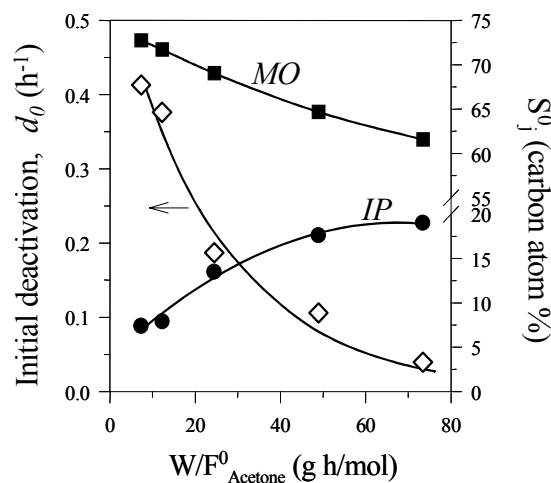


**Figure 8:** Initial catalyst deactivation and product selectivities as a function of contact time over MgO ( $T = 573$  K,  $P_{Acetone} = 7.7$  kPa)

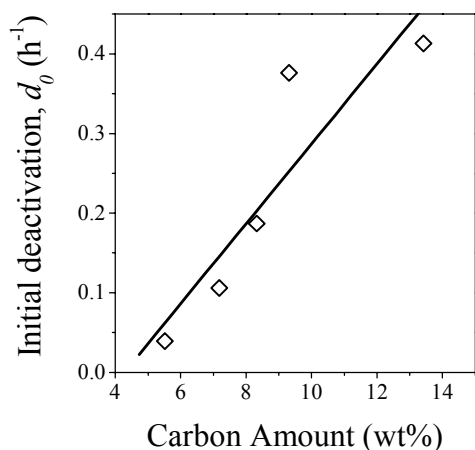


**Figure 9:** Initial catalyst deactivation as a function of the carbon amount deposited on MgO after 10-h catalytic runs at different contact times ( $T = 573 \text{ K}$ ,  $P_{\text{Acetone}} = 7.7 \text{ kPa}$ )

tetramethyltetralones ( $m/z = 202$ ) and other heavy polymers of  $m/z = 218$  and  $240$ .

Results can be explained by considering that the catalyst surface acid-base properties determine the preferential formation of a given trimeric intermediate which in turn defines both the formation of the product released to the gas phase (MO, IP or MES) and the nature of the carbon deposit. This interpretation is depicted in Figure 6. Coke formed from the 4,6-dimethylhepta-3,5-dien-2-one intermediate on acidic catalysts (dotted lines in Fig. 6) will be fundamentally aromatic in composition since MES can further react to xylenes and other  $C_{9+}$  aromatic hydrocarbons (Chang and Silvestri, 1977; Salvapati *et al.*, 1989). On the other hand, coke formed on more basic materials from phorone, will be mostly heavy  $\alpha,\beta$ -unsaturated ketones such as isoxylitones, tetralones and other  $C_{12+}$  oxygenates (Salvapati *et al.*, 1989; Lippert *et al.*, 1991). Then, the gradual shift from one intermediate to another causes a concomitant change in coke composition and it could explain the higher temperatures needed to burn the carbon deposits at increasing Al content in the samples, as observed in Fig. 5.

#### D. Relationship between catalyst deactivation and acid-base properties

The relative catalytic activity is defined as  $a = r_t / r_0$  where  $r_t$  and  $r_0$  are the reaction rates at time  $t$  and zero time respectively. Fig. 7 shows the activity decay of MgO as a function of time at different contact times. To quantify the effect of contact time on catalyst activity, the experimental points of Fig. 7 were fitted with first order deactivation functions and from the slopes of the curves, we calculated the initial deactivation rate as  $d_0 = [-da/dt]_{t=0}$ . A plot of the resulting  $d_0$  values as a function of contact time is presented in Fig. 8; it is observed that the initial deactivation rate decreases rapidly with increasing contact time. This result shows

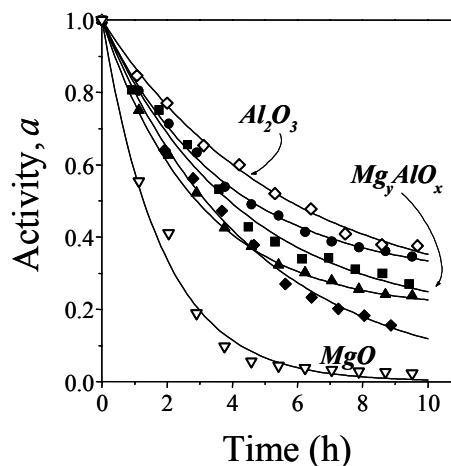


**Figure 10:** Acetone condensation activity as a function of time over  $Mg_yAlO_x$ , MgO and  $Al_2O_3$  catalysts ( $T = 473 \text{ K}$ ,  $P_{\text{Acetone}} = 7.7 \text{ kPa}$ ,  $W/F_{\text{Acetone}}^0 = 49 \text{ g h/mol}$ )  
 $\blacktriangle r = 0.11$ ;  $\bullet r = 0.18$ ;  $\circ r = 0.24$ ;  $\blacklozenge r = 0.47$

that the activity decline of MgO is not related to the formation of any terminal product in the consecutive reaction pathways. In Fig. 8 we also plotted the initial selectivities toward MO and the final product (IP) as a function of contact time. The fact that  $d_0$  parallels the MO selectivity dependence confirms that IP is not responsible for MgO deactivation. We can also discard water as responsible for deactivation of MgO since IP synthesis involves the concomitant formation of two water molecules; water partial pressure on the catalyst surface should therefore increase with increasing contact time, which is the opposite trend observed for  $d_0$  in Fig. 8. Then, the effect of water as a surface poison able to convert the Lewis acid sites ( $Mg^{2+}$ ) of MgO into inactive Mg-OH surface species can be neglected because although generation of these species *in situ* is possible, the labile nature of the surface bond probably makes them unstable under reaction conditions. In fact, we have shown previously by IR of  $CO_2$  the weak character of bicarbonate species formed on surface hydroxyls of MgO (Di Cosimo *et al.*, 1998b).

Since MO itself is not a strong coking agent (Reichle, 1980), it is reasonable to assume that on MgO coke may be formed from the unsaturated trimers as postulated in Fig. 6. Furthermore, in Fig 9 we present a linear correlation between the  $d_0$  values and the carbon amount measured by TPO after the catalytic runs of Fig. 7, indicating that the carbon deposit formed on the very active Mg-O pair sites causes the deactivation of the MgO catalyst.

Plots of the relative catalytic activity as a function of time on stream at 473 K (Fig. 10) showed that the activity decay on Mg-Al mixed oxides is faster than on  $Al_2O_3$  but slower than on MgO. Pure MgO presented a rapid deactivation and its residual activity after the 10-h run was very low. From the slope of the plots of Fig. 10, the initial deactivation rate was once more calculated. In Fig. 11, the  $d_0$  values obtained for all the

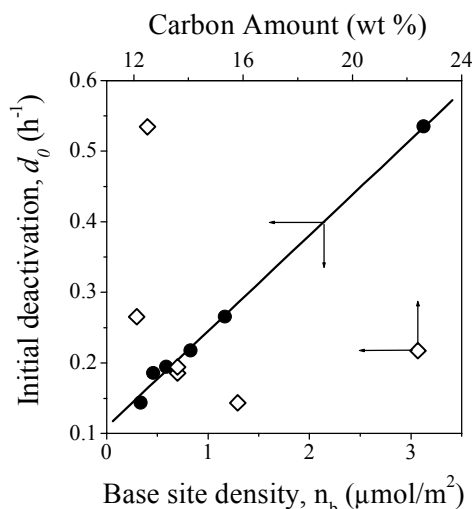


**Figure 11:** Initial catalyst deactivation of  $\text{Mg}_y\text{AlO}_x$  oxides,  $\text{MgO}$  and  $\text{Al}_2\text{O}_3$  as a function of the base site density and carbon amount deposited after 10-h catalytic runs ( $T = 473 \text{ K}$ ,  $P_{\text{Acetone}} = 7.7 \text{ kPa}$ ,  $W/F_{\text{Acetone}}^0 = 49 \text{ g h/mol}$ )

samples are represented in open symbols as a function of the carbon content measured after the catalytic runs (Table 2). Clearly, it does not exist any correlation between  $d_0$  and the amount of coke for  $\text{Mg}_y\text{AlO}_x$  catalysts, in contrast to what was obtained on pure  $\text{MgO}$  (Fig. 9). Initial deactivation is lower on  $\text{Al}_2\text{O}_3$  ( $d_0 = 0.14 \text{ h}^{-1}$ ) than on  $\text{MgO}$  ( $d_0 = 0.53 \text{ h}^{-1}$ ), in spite that alumina forms more coke during reaction and that the coke is more difficult to oxidize as compared to  $\text{MgO}$  (Table 2 and Fig. 5).

These results show that neither the coke amount nor its polymerization degree account for the catalyst deactivation order observed in Fig. 10. A better explanation is obtained by considering the nature of the surface sites that are responsible for the formation of coke precursors on pure  $\text{Al}_2\text{O}_3$  or  $\text{MgO}$ . Alumina contains Brønsted (OH groups) and Lewis (metal cations) acidic sites and probably coke forms preferentially on Brønsted sites rather than on Al-O acid-base pair sites. Contrarily to the known catalytic properties of Brønsted OH sites in liquid-phase heterogeneously catalyzed acetone aldolization at low temperatures, these sites are not active for the gas-phase reaction to unsaturated ketones and the reaction would proceed, therefore, at an appreciable rate on Al-O pairs even in the presence of a high carbon content deposited on the Brønsted sites.

Contrarily to what has been discussed above about disregarding the poisoning effect of water on  $\text{MgO}$ , we have no evidence on the role of water in poisoning Lewis acid sites of alumina. In fact, surface transformations caused by water leading to Al-H and Al-OH species with the consequent diminution of active surface Al-O pairs should be also taken into account in addition to coke formation when dealing with deactivation of alumina or Al-rich mixed oxides.

On  $\text{MgO}$ , the fast deactivation is due to the fact that aldolization and coke formation reactions compete for the same active site, the Mg-O pairs, thereby showing a linear correlation between  $d_0$  and the carbon amount (Fig. 9). The aldol reaction stops almost completely even when the carbon deposition is less intense than on Al-containing samples. On  $\text{Mg}_y\text{AlO}_x$  oxides, coke will mainly form on Mg-O pairs (Mg-rich samples) or Brønsted acid sites (Al-rich samples) following the Al content in the sample as shown in Fig. 6.

In Fig. 11, the  $d_0$  values obtained for  $\text{MgO}$ ,  $\text{Al}_2\text{O}_3$  and  $\text{Mg}_y\text{AlO}_x$  oxides were plotted as a function of the density of basic sites,  $n_b$  (Table 1). It is observed that the initial deactivation correlates linearly with the density of basic sites. No correlation was found between the  $\text{NH}_3$  site density ( $n_a$ , Table 1) and  $d_0$ . These results show that although  $\text{Mg}_y\text{AlO}_x$  oxides promote the self-condensation of acetone by both acid- and base-catalyzed pathways (Fig. 2), the initial deactivation rate is essentially related to the surface basic properties. This dependence of  $d_0$  with  $n_b$  for  $\text{Mg}_y\text{AlO}_x$  oxides probably reflects the fact that the acetone oligomerization rate decline is significantly higher when coke poisons very active Mg-O pair sites than when eliminates moderately active Al-O pair site because of the more basic features of the former.

#### IV. CONCLUSIONS

The activity and selectivity for acetone oligomerization on  $\text{Mg}_y\text{AlO}_x$  oxides depend on the catalyst acid-base properties, which in turn are determined by the aluminum content in the sample. Mg-rich catalysts selectively yield mesityl oxides whereas Al-rich  $\text{Mg}_y\text{AlO}_x$  oxides produce mainly isophorone.  $\text{Mg}_y\text{AlO}_x$  samples are more active than alumina. Intermediate Mg/Al compositions show unique catalytic properties because fulfill the reaction requirements for the density and strength of basic and acid sites.

The  $\text{Mg}_y\text{AlO}_x$  activity declines in the acetone oligomerization reaction due to a blockage of both basic and acidic active sites by a carbonaceous residue formed by secondary aldol condensation or hydrocarbon-forming reactions, respectively. The key intermediate species for coke formation are highly unsaturated linear trimers formed by aldol condensation of mesityl oxide with acetone that remain strongly bound to the catalyst surface. The catalyst surface acid-base properties determine the preferential formation of a given trimeric intermediate, which in turn defines the chemical nature of the carbon deposit. Aromatic hydrocarbons are the main component of coke formed on acidic Al-rich  $\text{Mg}_y\text{AlO}_x$  samples whereas heavy  $\alpha,\beta$ -unsaturated ketones preferentially form on basic Mg-rich catalysts.

Alumina forms more and heavier coke than  $\text{MgO}$  but the latter deactivates faster. This is explained by the fact that on  $\text{MgO}$  primary aldol condensation reactions and formation of coke precursors species take place on the same sites, i.e., the Mg-O pairs in which oxygen

presents moderate basic properties. In contrast, main reaction to ketones takes place on the Al-O pairs of alumina whereas  $\text{CH}_x$  coke precursors form on Brønsted OH groups that are inactive for aldol condensation reactions to unsaturated ketones.

Deactivation of  $\text{Mg}_y\text{AlO}_x$  oxides is caused by carbon deposition but neither the carbon amount nor its polymerization degree are key factors in terms of the deactivation rate. The nature of surface active sites for coke formation, which depend on the catalyst chemical composition, seems to define the activity decay rate.

Deactivation of  $\text{Mg}_y\text{AlO}_x$  oxides during acetone oligomerization reactions is essentially related to the surface basic properties. This is because the activity decline is significantly higher when coke poisons very active basic Mg-O pairs than when eliminates moderately active acidic Al-O pairs.

#### Acknowledgements

Support of this work by the Consejo Nacional de Investigaciones Científicas y Técnicas (CONICET), Argentina and by the Universidad Nacional del Litoral, grant CAI+D 94-0858-007-049, Santa Fe, Argentina, is gratefully acknowledged.

#### REFERENCES

- Berteau, P., B. Delmon, J.L. Dallons and A. Van Gysel, "Acid-base properties of silica-aluminas: use of 1-butanol dehydration as a test reaction", *Appl. Catal.* **70**, 307-323 (1991).
- Chang, C.D. and A.J. Silvestri, "The conversion of methanol and other O-compounds to hydrocarbons over zeolite catalysts", *J. Catal.* **47**, 249-259 (1977).
- Di Cosimo, J.I., V.K. Díez and C.R. Apesteguía, "Base catalysis for the síntesis of  $\alpha,\beta$ -unsaturated ketones from the vapor-phase aldol condensation of acetone", *Appl. Catal.* **137**, 149-166 (1996).
- Di Cosimo, J.I. and C.R. Apesteguía, "Study of the catalyst deactivation in the base catalyzed oligomerization of acetone", *J. Molec. Catal.* **130**, 177-185 (1998).
- Di Cosimo, J.I., V.K. Díez and C.R. Apesteguía, "Synthesis of  $\alpha,\beta$ -unsaturated ketones over thermally activated Mg-Al hydrotalcites", *Appl. Clay Science* **13**, 433-449 (1998a).
- Di Cosimo, J. I. , V. K. Díez, M. Xu, E. Iglesia and C. R. Apesteguía, "Structure and Surface and Catalytic Properties of Mg-Al basic oxides", *J. Catal.* **178**, 499-510 (1998b).
- Di Cosimo, J.I., C.R. Apesteguía, M.J.L. Ginés and E. Iglesia, "Structural requirements and reaction pathways in condensation reactions of alcohols on  $\text{Mg}_y\text{AlO}_x$  catalysts", *J. Catal.* **190**, 261-275 (2000).
- Garrone, E. and F. Stone, "UV diffuse reflectance spectra of ammonia adsorbed on alkaline earth oxides and analogy with charge-transfer-to-solvent spectra", in M. Che and G.C. Bond (Eds.), *Adsorption and Catalysis on Oxide Surfaces*, Elsevier, Amsterdam (1985).
- Lippert, S., W. Baumann and K. Thomke, "Secondary reactions of the base-catalyzed aldol condensation of acetone", *J. Molec. Catal.* **69**, 199-214 (1991).
- Prinetto, F., G. Ghiotti, R. Durand and D. Tichit, "Investigation of acid-base properties of catalysts obtained from layered double hydroxides", *J. Phys. Chem. B* **104**, 11117-11126 (2000).
- Reichle, W.T., "Pulse microreactor examination of the vapor-phase aldol condensation of acetone," *J. Catal.* **63**, 295-306 (1980).
- Reichle, W.T., "Catalytic reactions by thermally activated, synthetic, anionic clay minerals", *J. Catal.* **94**, 547-557 (1985).
- Salvapati, G.S., K.V. Ramanamurty and M. Janardanao, "Selective catalytic self-condensation of acetone", *J. Molec. Catal.* **54**, 9-30 (1989).
- Velu, S. and C.S. Swamy, "Kinetics of the alkylation of phenol with methanol over magnesium-aluminium calcined hydrotalcites", *Appl. Catal.* **145**, 225-230 (1996).

Received: September 16, 2001.

Accepted for publication: July, 26, 2002.

Recommended by Guest Editors J. Cerdá, S. Díaz and A. Bandoni.